

## DYNAMIC PRECIPITATION IN Al-Mg- AND Al-Mg-Si ALLOYS

Tanja Pettersen, Katrin Nord-Varhaug and Erik Nes

Dept. of metallurgy, Norwegian University of Science and Technology,  
N-7034 Trondheim, Norway

### ABSTRACT

Hot torsion of three different aluminium alloys has been performed. Two Al-Mg-Si alloys and one Al-Mg alloy, given different homogenisation treatments, was investigated. An important issue has been to investigate the effect of homogenisation treatment on the flow stress. It was found that increasing the strain rate at a constant Zener-Hollomon parameter ( $Z$ ) gave decreasing values for the flow stress, the variation in flow stress was measured to be over 30MPa at most. The reason for this unexpected behaviour was attributed to a phenomenon referred to as dynamic precipitation. TEM-investigations of the materials revealed different subgrain structure in the specimens deformed at high and low strain rates (constant  $Z$ ).

**Keywords:** *Dynamic precipitation, effect of homogenisation, Mg<sub>2</sub>Si-precipitation.*

### 1. INTRODUCTION

The classical way to study precipitation-hardened alloys comprise annealing of material in which the precipitating elements in advance is brought into solid solution. This annealing treatment involve nucleation and growth of precipitates, a process referred to as static precipitation. In material containing magnesium and silicon atoms, Mg<sub>2</sub>Si particles will nucleate at temperatures below the solvus temperature. This process is relatively time consuming in the static case. When hot deformation of materials with precipitating elements in solid solution is carried out below the solvus temperature, precipitation will occur and will be strongly influenced by the deformation. The particles nucleate at the moving dislocations, and as a result the precipitating reaction happens at a much higher rate. This phenomenon is referred to as dynamic precipitation. Dynamic precipitation requires that there is precipitating elements in solid solution and in addition that the time of the test is sufficiently long for precipitation to occur.

### 2. EXPERIMENTAL

Most of the investigations were carried out on a 5005-alloy (0.88wt% Mg, 0.12wt% Si, 0.08wt% Mn, 0.27wt% Fe, balance Al), but supplementary experiments were also carried out on a 6082-alloy (0.65wt% Mg, 0.99wt% Si, 0.47wt%Mn, 0.21wt% Fe, balance Al) and a 6060-alloy (0.48wt% Mg, 0.43wt% Si, 0.02wt% Mn, 0.20wt% Fe, balance Al). Before deformation the materials were homogenised using two different procedures:

(I) : Heating at a rate of 200°C/hour to a final temperature of 580°C, held at this temperature for 3 hours and water-quenched immediately afterwards.

(IV) : The specimens were heated to a temperature of 580°C at a rate of 200°C/hour, and held at this temperature for 3 hours. Then the specimens were cooled to a temperature of 480°C at a rate of 200°C/hour, and held at this temperature of 1 hour, further cooled at a rate of 50°C/hour to a temperature of 430°C, and held at this temperature for 4 hours, further cooled at a rate of 50°C/hour to a temperature of 400°C and held at this temperature for 72 hours. Then cooled at a rate of

50°C/hour to a temperature of 350°C and held at this temperature for 66 hours and finally slowly cooled in air.

Hot torsion tests has been carried out in the temperature range from 233°C to 600°C and at strain rates ranging from 0.01/s to approximately 15/s. The temperature recorded during heating up and deformation is measured by a thermocouple placed in the centre of the specimen. The difference in temperature at the surface and in the centre of the torsion specimen was measured for different temperatures, and is accounted for in the results. At high strain rates the temperature is also compensated for temperature rise due to adiabatic heating, which is a good first approximation if the time of the test is short. The temperatures and strain rates were combined so that only four different Zener-Hollomon parameters were investigated. The specimens were heated by induction to the deformation temperature, and then held at this temperature for 300s before deformation. After deformation the specimens were immediately quenched in water. After hot torsion some of the 5005-specimens were investigated in a Philips CM30 TEM. The specimens were cut in a section parallel to the torsion axis to a maximum thickness of about 1200µm, and then ground from both sides to a thickness of less than 100µm, and finally electropolished.

### 3. RESULTS

The results from the torsion experiments are displayed in Figure 1 and 2, Figure 1 showing the specimens quenched after homogenisation and Figure 2 showing the specimens slowly cooled. For both homogenisation treatments experiments were carried out at a constant Zener-Hollomon parameter, varying the strain rate from 0.01/s to 15/s and varying the temperature to compensate for the change in strain rate. In Figure 1 it can be seen that at the highest Zener-Hollomon parameters the flow stress decrease with increasing strain rate and there is a drop in flow stress of more than 30MPa for a constant Z. At the lower Z-values, which corresponds to specimens deformed at higher temperatures, there are only minor changes in peak flow stress. In Figure 2 the high and low strain rate experiments (0.01/s and 15/s) are repeated with specimens given homogenisation treatment IV, and it can be seen that the specimens deformed at the low and the high strain rates gives nearly identical peak flow stresses.

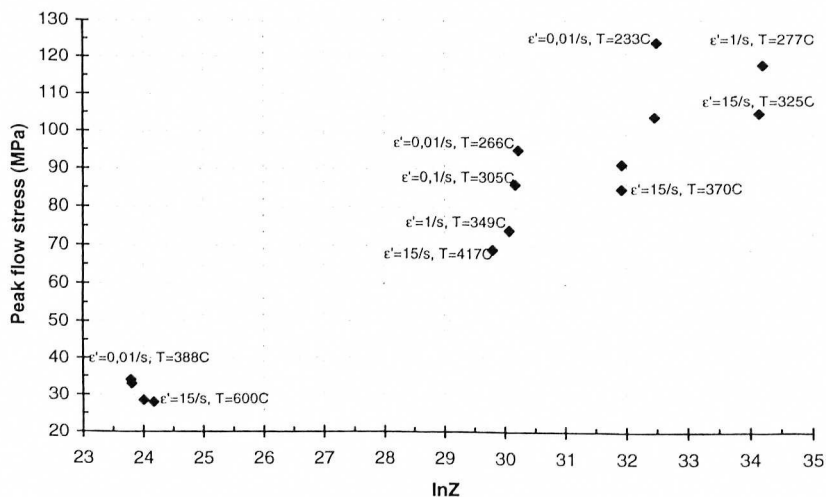


Figure 1: Peak flow stress as a function of Zener-Hollomon parameter. The experiments are performed on the 5005-alloy. The specimens were quenched after homogenisation (treatment I).

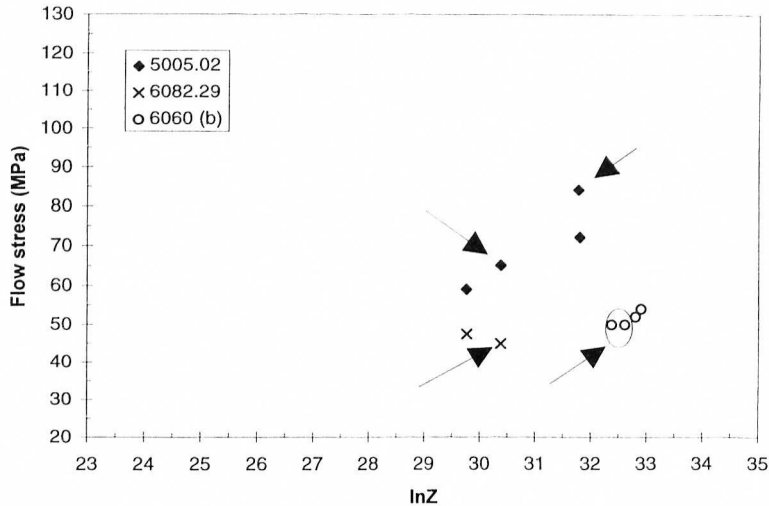


Figure 2: Flow stress plotted as a function of  $\ln Z$ . As indicated, the figure contains results from three different alloys; 5005, 6082.29 and 6060. All the specimens were given homogenisation treatment IV, and deformed at strain rates of 15/s and 0.01/s. The arrows mark experimental results where the strain rate is 0.01/s.

To further investigate these observations, thin foils were made from the specimens deformed at both high and low strain rates, and from both homogenisation treatments. Table 1 summarise the various deformation conditions investigated in the TEM, and results from the TEM investigations are shown in Figures 3 and 4. Figure 3a) and 3b) shows micrographs from specimens deformed at a strain rate of 15/s and at a temperature of 400°C and given different homogenisation treatments before deformation. The material quenched after homogenisation was found to have slightly smaller subgrains ( $\bar{\delta}=1\mu\text{m}$ , mean intercept length) than the material given homogenisation treatment IV ( $\bar{\delta}=1.1\mu\text{m}$ , mean intercept length). In the quenched material some of the subgrains also contained a tangled network of dislocations in the interior of the subgrains. This was not found to the same extent in the material slowly cooled after homogenisation.

Table 1: Deformation conditions for the specimens investigated in TEM. When calculating  $Z$  an activation energy of 156kJ/mol has been used.  $\dot{\epsilon}$  is the strain rate.

Homog.	$Z$ (1/s)	Temp. (°C)	$\dot{\epsilon}$ (1/s)
I and IV	$1.9 \cdot 10^{13}$	400	15
I and IV	$1.3 \cdot 10^{13}$	266	0.01

Figure 4 shows the material deformed at a slow strain rate. The material quenched after deformation (Figure 4a) contained flat, pancake-shaped subgrains, and the mean subgrain intercept length for this material was measured to be  $0.5\mu\text{m}$  in the normal direction and  $0.8\mu\text{m}$  in the shear direction. In the material slowly cooled after homogenisation (Figure 4b), the subgrains were equiaxed, and the mean subgrain intercept length was measured to be  $1\mu\text{m}$ , and an inhomogeneous subgrain structure was observed. Investigations of the particle structure resulting from the different homogenisation treatments showed small particles, about 15-20nm in diameter, in the material quenched after homogenisation. The particles were attached to dislocations, bowing out between the particles. The particles in the material slowly cooled was measured to be  $\sim 10$  times as large, and not having the same effect on the dislocations.

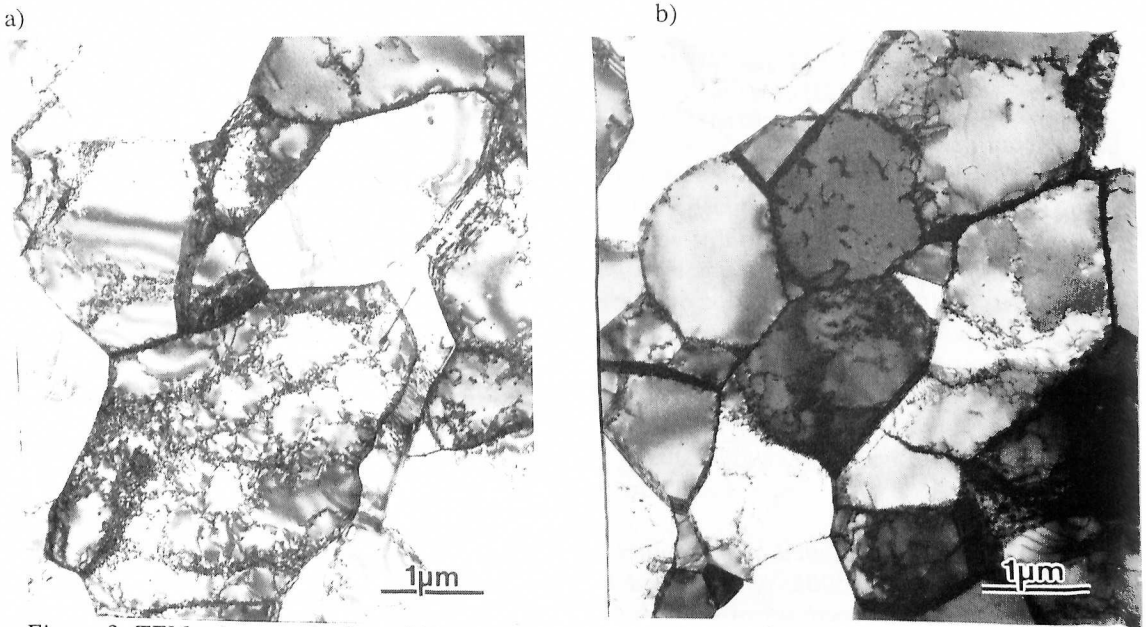


Figure 3: TEM-micrographs from 5005-torsion specimens deformed at a strain rate of 15/s and at a temperature of 400 °C. a) This material was quenched after homogenisation and the peak flow stress of the specimen was measured to be 69MPa. b) This material was given homogenisation treatment IV before deformation, and the peak flow stress was measured to be 59MPa.

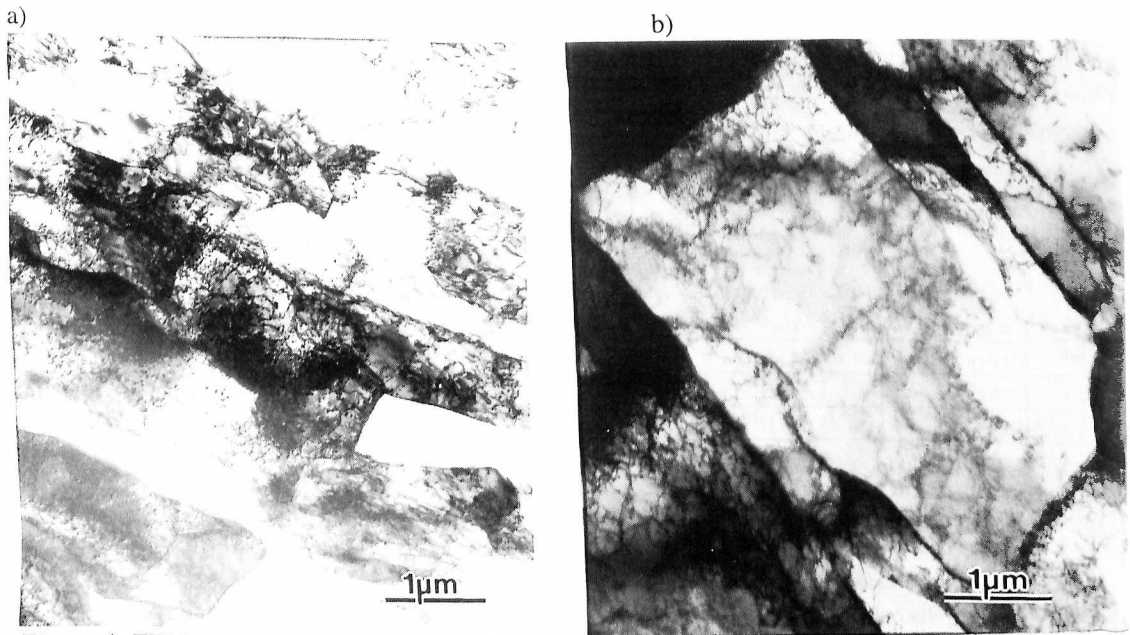


Figure 4: TEM-micrographs from 5005-torsion specimens deformed at a strain rate of 0.01/s and a temperature of 266 °C. a) Shows a specimen quenched after homogenisation, the peak flow stress was measured to be 98MPa. b) Shows a specimen which has been given homogenisation treatment IV before deformation, the peak flow stress was measured to be 65MPa.

#### 4. DISCUSSION

In material quenched after deformation and subsequently deformed at a low temperature and strain rate, the resulting peak flow stress is higher than in material deformed at the same  $Z$  but at higher strain rate. This can be accounted for in the following way: In both samples there is an excess of precipitating elements in solid solution before torsion, deforming the sample at a low strain rate below the solvus temperature the precipitating elements will nucleate at the moving dislocations, and the formed particles will act as obstacles to the moving dislocations and the flow stress increases. At a high strain rate the deformation is finished in a relatively short time interval, and the reaction rate of the precipitation is too low to effect the flow stress to the same extent. This explanation of the variation in flow stress shown in Figure 1 is confirmed by the experiments displayed in Figure 2. Giving the material a heat treatment to drain away the precipitating elements gives similar results for the samples deformed at high and low strain rates. In this figure results from heat treatable alloys are also included, giving similar results. Note also a slight decrease in flow stress for the 5005-(IV) specimen deformed at the highest strain rate compared to the (I)-specimen. This indicates that even at the highest strain rate there is some precipitation during deformation. For the lowest strain rates there is a large effect of bringing the precipitating elements into solid solution.

In the 5005-alloy the content of precipitating elements are relatively low. For comparison experiments was also carried out on a 6060-alloy and a 6082-alloy. In the experiments performed on the 6060-alloy given homogenisation treatment (I) an increase in peak flow stress of 40MPa was observed at  $Z=1.9 \cdot 10^{13}/s$  (lowest strain rate=0.01/s and highest strain rate=15/s). That is, the increase in flow stress due to dynamic precipitation in this material is about 10MPa higher than in the 5005-alloy. For alloys 6082 and 6060 given homogenisation treatment (IV), there was almost no variation in peak flow stress at the same  $Z$ , an observation which again confirms the idea of dynamic precipitation in the previous case. For alloy 5005 the flow stress range has decreased, but is still present. At  $\ln Z=32$ , the flow stress range is about 10MPa while for the water quenched materials the range is about 40MPa. The most reasonable interpretation is that this alloy still have Mg/Si in supersaturation in significant amount to cause dynamic precipitation.

The flow stress in this material can be expressed as a sum of the contribution from the dislocations stored in the interior of the subgrains and in the subgrain walls in addition to the contribution from the particles.

$$\tau = \tau_i + \tau_p + \alpha_1 Gb\sqrt{\rho_i} + \alpha_2 Gb \frac{1}{\delta} \quad (1)$$

$\tau_i$  is the frictional stress,  $\tau_p$  is the flow stress contribution from the particles,  $\alpha_1$  and  $\alpha_2$  are constants,  $G$  is the shear modulus,  $b$  is Burgers vector,  $\rho_i$  is the density of dislocations in the cell interior and  $\delta$  is the cell/subgrain size.

The subgrain size in the material shown in Figure 3a) was measured to be  $1\mu m$  corresponding to a flow stress of 69MPa. By reducing the supersaturation of magnesium and silicon atoms prior to deformation the flow stress at the same deformation conditions reduces with about 14% to a flow stress of 59MPa. At the same time the subgrain size increases to a value of  $1.1\mu m$ , which corresponds to a change in the last part of Eq. (1) by about 10%. This indicates that the change in flow stress is due to both the change in  $\tau_p$  and the change in the dislocation structure caused by the change in particle structure. The smaller subgrain size in material quenched after homogenisation is

probably due to that the small particles precipitated during deformation will restrain the dynamic recovery in the material, giving a higher density of stored dislocations. In Figure 4 the same phenomenon is shown for material deformed at a lower strain rate. The flow stress changes from a value of 98MPa in the material quenched after deformation to a value of 65MPa in the material slowly cooled. This is a decrease of 33%. At the same time the mean subgrain size increases with 30% from a mean value of 0.7 $\mu$ m (calculated by using  $\bar{\delta} = \sqrt[3]{\delta_{RD}^2 \cdot \delta_{ND}}$ ) to a mean value of 1 $\mu$ m. The decrease in peak flow stress, and the corresponding increase in subgrain size is larger in the materials deformed at the lowest strain rate. At the lowest strain rate the time of the deformation is 150seconds, giving the precipitation reactions time to occur, while the deformation at a strain rate of 10/s is over in 0.15seconds. Which implies that the density of particles is higher in the materials deformed at the lowest strain rates, this was qualitatively confirmed by the TEM studies.

From Equation (1) it can be seen that the particles contribute to the flow stress in two ways; (i) by the direct contribution  $\tau_p$ , and (ii) the particles indirectly contribute to the flow stress by changing the dislocation structure in the material. In addition to changing the subgrain size as discussed above, the particles also changes the structure of the interior dislocations. The material shown in Figure 3a) contained a network of tangled dislocations, giving a structure of poorly defined cell boundaries in addition to the more well defined subgrain boundaries. The same material also show areas with a high density of dislocations not arranged in subgrain or cell boundaries. This is also shown in Figure 4a), but in this material the interior dislocation density is much higher, making the distinction of the individual dislocations difficult. A closer look at this material shows that the interior dislocations are pinned down by the small particles (of diameter 15-20nm). The large particles does not interact with the dislocations in the same way, and the microstructure in material in which the supersaturation of Mg and Si is removed before deformation is clearer, with well defined subgrain boundaries and relatively few interior dislocations.

## 5. CONCLUDING REMARKS

It has been found that increasing the strain rate at a constant Z gave decreasing values for the flow stress in material with an excess of elements in solid solution. This effect is found be due to precipitation during deformation and it disappears when the precipitating elements are removed from solid solution. Two homogenisation treatments has been investigated, one in which the material is quenched after homogenisation and the other in which the material is slowly cooled after homogenisation. A considerable contribution to the change in peak flow stress is found to be due to the change in the dislocation structure.

## ACKNOWLEDGEMENTS

The authors wish to acknowledge Hydro Aluminium for financial support and for supplying the materials

## REFERENCES

- [1] Blaz L., Evangelista E., Niewczas M., Met. trans. A, **25A**, (1994), 257.
- [2] Cerri E., Evangelista E., Ryum N., Met. Trans. A, **27A**, (1996), 2916.
- [3] Evangelista E., Forcellese A., Gabrielli F., Mengucci P., Int. J. Mat. Prd. Technol., **5**, (1990), 84.
- [4] Usui E., Inaba T., Shinano N., Z. Metallkde., **76**, (1985), H.6, 426.
- [5] Usui E., Inaba T., Shinano N., Z. Metallkde., **76**, (1985), H.12, 786.
- [6] Usui E., Inaba T., Shinano N., Z. Metallkde., **77**, (1986), H.3, 179.